Journal of Magnetism and Magnetic Materials 428 (2017) 43–49

Contents lists available at ScienceDirect

Journal of Magnetism and Magnetic Materials

journal homepage: www.elsevier.com/locate/jmmm

Magnetic and XMCD studies of $Pr_{1-x}Sr_xMnO_3$ manganite films

Yu.E. Samoshkina[a,*], I.S. Edelman[a], E.A. Stepanova[b], D.S. Neznakhin[b], K. Ollefs[c], N.V. Andreev[d], V.I. Chichkov[d]

[a] Kirensky Institute of Physics, Federal Research Center KSC SB RAS, Krasnoyarsk 660036, Russia
[b] Ural Federal University, Yekaterinburg 620000, Russia
[c] European Synchrotron Radiation Facility (ESRF), BP 220, 38043 Grenoble Cedex 9, France
[d] National University of Science and Technology "MISiS", Moscow 119049, Russia

ARTICLE INFO

Keywords:
Hole-doped manganites
Thin films
Magnetic measurements
Spin-glass behavior
X-ray magnetic circular dichroism

ABSTRACT

Magnetic properties of the $Pr_{0.8}Sr_{0.2}MnO_3$ and $Pr_{0.6}Sr_{0.4}MnO_3$ polycrystalline films have been studied using temperature and magnetic field dependences of the static magnetization and X-ray magnetic circular dichroism (XMCD) spectroscopy. For the both compositions, the difference between the temperature dependences of magnetization obtained in the zero fields cooling (ZFC) and field cooling (FC) modes has been revealed. The ZFC curves demonstrate a pronounced maximum at temperature T_m. It is shown that the T_m value dependence on the magnetic field follows the Almeida-Thouless line typical for the classic spin glass, what allows us to assume the possible spin-glass behavior of the films. Effect of the disorder in a direction of the crystallites easy-axis on the difference between FC and ZFC curves has been discussed also. Magnetic field dependences of the sample magnetization are presented by the hysteresis loops with the shape changing upon temperature variation. This behavior has been attributed to the effect of crystallographic anisotropy and Pr ions. The spectra and magnetic field dependences of XMCD at the Pr L_2- and Mn K-edges have been studied at 90 K. The magnetic field dependences of the XMCD at the Pr L_2-edge had shown Van Vleck paramagnetism from Pr^{3+} ions.

1. Introduction

Since the discovery of the colossal magnetoresistance effect in the hole-doped manganites with the chemical formula $R_{1-x}M_xMnO_3$, where R is the trivalent lanthanide (La, Pr, Dy, etc.) and M is the divalent alkaline earth metal (Sr, Ca, Pb, Ba) [1,2], these materials are among the main objects of research in physics of magnetic phenomena [3–6]. The parent $RMnO_3$ compound is known to be a Mott insulator with the antiferromagnetic (AFM) ground state caused by the indirect exchange coupling between Mn^{3+} ions through the O^{2-} ions introduced by Kramers [7] and now known as a "super-exchange".

The ferromagnetic (FM) state caused by the partial replacement of lanthanide ions by divalent alkaline earth ions is related to the exchange coupling between Mn^{3+} and Mn^{4+} ions and described in the framework of the double exchange model proposed by C. Zener [8,9]. Depending on the x value, the pure FM or AFM magnetic state as well as the intermediate magnetic state caused by phase separation of a sample into FM and AFM regions can be observed in a substituted manganite. In particular, the competition between the FM and AFM exchange couplings leads to the formation of specific magnetic states in a sample, including spin-glass or cluster spin-glass ones [10] which were observed in ceramic materials, single crystals, and films [11]. All these circumstances make the study of the magnetic properties of the doped manganites to be greatly demanded. Historically, the $La_{1-x}Sr_xMnO_3$ compounds have been the most intensively investigated of Sr-doped manganites. A few works were devoted to the magnetic and transport properties of single-crystal and polycrystalline Pr-Sr manganites [12–18]. Special attention was paid to the effect of deviations from the stoichiometric composition on the magnetic and transport properties of $Pr_{1-x}Sr_xMnO_3$ (PSMO) compounds. In Refs. [19–22], the possible contribution of rare-earth (e.g., Tb, Dy, or Pr) spins in the magnetic properties of manganites was considered. In our previous work [23], we studied visible magnetic circular dichroism (MCD) spectra of the PSMO thin films with x=0.2 and x=0.4 and revealed the different temperature dependences of the intensity of the MCD maxima observed in different parts of the investigated spectrum. For manganites, this phenomenon was observed for the first time. Since the MCD effect should be proportional to the magnetization of a sample, the magnetic measurements are of the primary important for further investigation of the PSMO films.

This paper is focused on a detailed study of the temperature and magnetic field dependences of magnetization of the $Pr_{1-x}Sr_xMnO_3$

* Corresponding author.
E-mail address: uliag@iph.krasn.ru (Y.E. Samoshkina).

http://dx.doi.org/10.1016/j.jmmm.2016.12.014
Received 2 July 2016; Received in revised form 4 October 2016; Accepted 4 December 2016
Available online 06 December 2016

(x=0.2 and x=0.4) polycrystalline films with different thicknesses. Static magnetic measurements were performed in wide temperature and magnetic field intervals at the parallel and perpendicular field orientations relative to the film plane. Besides, X-ray magnetic circular dichroism (XMCD) at Mn K- and Pr L_2- edges in varying magnetic field was investigated. XMCD in the absorption of X-rays gives an additional information comparing to the magnetic and visible MCD measurements because the XMCD signal arises at atomic core level absorption edges, and is therefore element-specific, what allows to separate magnetic properties of different atomic species in compounds [24].

2. Materials and methods

Films with a thickness ranging from 50 to 150 nm were prepared by the dc magnetron sputtering with the "facing-target" scheme [25,26]. This scheme allows transferring elements from a target to a substrate without changes in the composition. Therefore sputtering could be carried out from stoichiometric single phased $Pr_{0.8}Sr_{0.2}MnO_3$ and $Pr_{0.6}Sr_{0.4}MnO_3$ targets fabricated by the solid-state synthesis from stoichiometric Pr_2O_3, SrO, and MnO_2 powders. Before sputtering, the residual pressure in a vacuum chamber was 3×10^{-6} Torr. The operating pressure of the Ar and O_2 gas mixture (4:1) was 3×10^{-3} Torr. Thin films were grown on (311) YSZ (yttrium stabilized zirconium oxide) substrates. The substrate temperature during sputtering was 750 °C.

The analysis of the studied samples using the Rutherford backscattering method showed that the films thickness corresponds to the declared, and their chemical composition corresponded to the claimed stoichiometry. The crystal structure and phase purity of the samples were examined earlier using room-temperature powder X-ray diffraction (XRD) with Cu$K\alpha$ radiation [23]: samples with x=0.2 and 0.4 showed high peaks corresponding to the YSZ substrate and a series of relatively narrow low-intensity peaks corresponding to the only one polycrystalline phase – $Pr_{0.8}Sr_{0.2}MnO_3$ or $Pr_{0.6}Sr_{0.4}MnO_3$, correspondingly - without a pronounced texture. The crystal structure was refined within the orthorhombic $Pnma$ space group with the lattice parameters and average crystallite size given in Table 1. Structural parameters of the films were consistent with the data for bulk $Pr_{0.8}Sr_{0.2}MnO_3$ and $Pr_{0.6}Sr_{0.4}MnO_3$ samples [12–15].

Magnetic measurements were performed using a Quantum Design MPMS-XL7 EC SQUID magnetometer in the temperature range 5–300 K and magnetic fields of up to 20 kOe applied parallel or perpendicular to the film plane.

X-ray magnetic circular dichroism (XMCD) experiments at Pr L_2 – and Mn K-edges were carried out at the ID12 beamline of the European Synchrotron Radiation Facility in the total fluorescence yield mode at the grazing (15°) incidence of the X-ray beam. The XMCD spectra were obtained for the thickest films (130 and 150 nm for x=0.2 and x=0.4, respectively) as a difference between absorption spectra measured in the right- (μ+) and left-hand (μ−) circularly polarized light at the temperature T=90 K and magnetic field H =10 kOe applied along the beam direction.

Table 1
Structural parameters and crystallites size of PSMO films.

Film	$Pr_{0.8}Sr_{0.2}MnO_3$	$Pr_{0.6}Sr_{0.4}MnO_3$
Space group	*Pnma*	*Pnma*
a, Å	5.480 (1)	5.4465 (7)
b, Å	7.761 (1)	7.721 (1)
c, Å	5.462 (5)	5.422 (1)
V, Å^3	232.3 (2)	228.00 (6)
Average crystallites size, nm	31 (3) along b axis 54 (4) along a and c axes	45 (7) along b axis 62 (3) along a and c axes

3. Results

3.1. Temperature dependences of magnetization

Typical temperature dependences of magnetization M (T) for the PSMO films with x=0.2 and x=0.4 are shown in Fig. 1a and b, respectively. Measurements were made for the field cooling (FC) and zero field cooling (ZFC) modes in the course of samples heating in external magnetic fields (H) of different values and orientations relative to the film plane - parallel and perpendicular. The magnetization is expressed as μ_B/formula unit (f.u.), according to the formula

$$\mu_B/f.\,u. = \frac{M^*\sigma}{N_A{}^*\mu_B}, \quad (1)$$

where M is the molar mass of a substance (g/mole), σ is the sample magnetization (emu/g), N_A is the Avogadro number, and μ_B is the Bohr magneton (erg/G). In the experiments, magnetization was determined in the emu/cm^3 units. To express magnetization in the emu/g units, we assumed the film density to be equal to the density of the corresponding single crystal: ρ=6.667 g/cm^3 for $Pr_{0.8}Sr_{0.2}MnO_3$ and ρ=6.469 g/cm^3 for $Pr_{0.6}Sr_{0.4}MnO_3$.

First, let us consider the FC curves. A sharp increase in the magnetization with a decrease in temperature from the Curie temperature (T_C) to approximately 100 K is characteristic of the $Pr_{0.8}Sr_{0.2}MnO_3$ films and consistent with the behavior of bulk samples of the same composition [12,13]. For the $Pr_{0.6}Sr_{0.4}MnO_3$ films, an increase in the magnetization with decreasing temperature is not as sharp as for bulk crystals of the same composition [14,15]. In addition, the features observed at temperatures of 75 K in Ref. [14] and of 100 K in Ref. [15] and the temperature hysteresis near these temperatures in the FC curves for the bulk $Pr_{0.6}Sr_{0.4}MnO_3$ single and polycrystalline samples, correspondingly, are missing here. Note that these features were not observed also by other authors who investigated stoichiometric $Pr_{0.6}Sr_{0.4}MnO_3$ polycrystals [18]. The T_C values for the $Pr_{0.8}Sr_{0.2}MnO_3$ and $Pr_{0.6}Sr_{0.4}MnO_3$ films (Tables 2 and 3) are about 120 and 250 K, respectively, which is noticeably lower than the T_C values for bulk polycrystalline PSMO (170 and 310 K) [13,15].

The obtained FC and ZFC curves diverge at temperature T_{irr} that is called usually the irreversibility temperature. At $T < T_{irr}$, the ZFC curves are located below the FC curves and have a broad maximum centered at certain temperature T_m, after which magnetization decreases with temperature approaching the zero value. In the high-temperature region, the ZFC and FC curves merge with each other. It was found that the temperatures T_{irr} and T_m as well as the maximum width depend on the external magnetic field value and orientation. As a rule, these temperatures decrease with increasing magnetic field. In the maximal applied magnetic field (H=3 kOe) directed parallel to the sample plane, the FC and ZFC curves coincide with each other over the entire temperature range for both film compositions (squares in Fig. 1a and b). However, in the same magnetic field directed perpendicular to the sample plane, the FC and ZFC curves discrepancy persists (triangles in Fig. 1a and b).

3.2. Magnetic field dependences of magnetization

Magnetization dependences on an external magnetic field, H, obtained for the $Pr_{0.8}Sr_{0.2}MnO_3$ and $Pr_{0.6}Sr_{0.4}MnO_3$ films of 150 nm and 130 nm in thickness, respectively, at two mutually perpendicular H orientations relative to the film plane are shown in Fig. 2a and b. Symmetric hysteresis loops were observed at 5 K for all samples. The coercivity H_C and the saturation magnetization M_s depend on the film thickness (Tables 2 and 3) but do not depend on the H orientation, analogous to the case of $La_{0.7}Sr_{0.3}MnO_3$ films investigated earlier [27]. The saturation magnetizations estimated from the magnetization curves obtained in the in-plane field (Fig. 2a

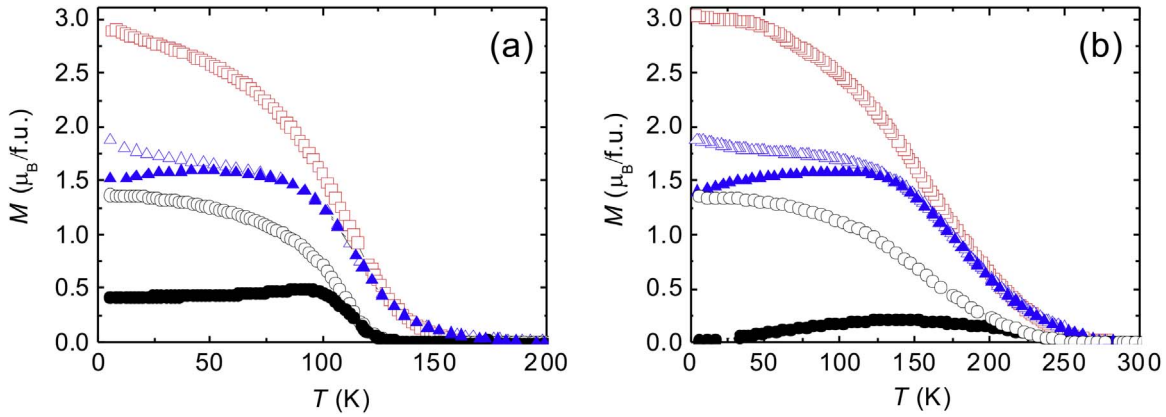

Fig. 1. FC (open symbols) and ZFC (closed symbols) magnetization curves vs temperature for (a) $Pr_{0.8}Sr_{0.2}MnO_3$ and (b) $Pr_{0.6}Sr_{0.4}MnO_3$ films (150 and 130 nm in thickness, correspondingly). The field H=3 kOe is parallel (squares) and perpendicular to the film plane (triangles); the field H=100 Oe is parallel to the film plane (circles).

Table 2
Experimental data of the $Pr_{0.8}Sr_{0.2}MnO_3$ films obtained in the magnetic field directed parallel to the sample plane: Curie temperature (T_C); coercive field (H_C), value of the saturation magnetization (M_s), normalized remanent magnetization (M_r/M_s), and demagnetizing field ($4\pi M_s$) at 5 K.

Thickness (nm)	T_C (K)	H_C (Oe)	M_s (μ_B/f.u.)	M_r/M_s	$4\pi M_s$ (kOe)
50	120	765	2.46	0.51	4.9
100	120	618	2.72	0.47	5.4
150	120	574	3	0.435	6

Table 3
Experimental data of the $Pr_{0.6}Sr_{0.4}MnO_3$ films obtained in the magnetic field directed parallel to the sample plane: Curie temperature (T_C); coercive field (H_C), value of the saturation magnetization (M_s), normalized remanent magnetization (M_r/M_s), and demagnetizing field ($4\pi M_s$) at 5 K.

Thickness (nm)	T_C (K)	H_C (Oe)	M_s (μ_B /f.u.)	M_r/M_s	$4\pi M_s$ (kOe)
50	250	886	2.54	0.6	5.2
80	250	613	2.87	0.58	5.8
130	250	424	3.24	0.56	6.6

and b) at T=5 K are M_s~3 μ_B/f.u. for $Pr_{0.8}Sr_{0.2}MnO_3$ (150 nm) and M_s~3.2 μ_B/f.u. for $Pr_{0.6}Sr_{0.4}MnO_3$ (130 nm). The loop rectangularity was determined as M_r/M_s, where M_r is the remnant magnetization. The obtained values are given in Tables 2 and 3.

With the temperature increase, the shape of the magnetization curves changes and H_C decreases sharply. The examples at T=90 K are shown in Fig. 2a and b (squares) for $Pr_{0.8}Sr_{0.2}MnO_3$ and $Pr_{0.6}Sr_{0.4}MnO_3$ films, correspondingly. One can see that the hysteresis almost vanishes and the magnetization curve consists of two linear portions with different slopes in the magnetic field intervals 0–1 kOe and 1–20 kOe. The shape of the magnetization curves changes beginning with ~25 K. The temperature dependence of coercivity H_C for the $Pr_{0.6}Sr_{0.4}MnO_3$ film (130 nm) in the in-plane magnetic field is shown in the inset in Fig. 3. For all other samples, the analogous picture is observed.

3.3. X-ray magnetic circular dichroism

As it was mentioned in the introduction, XMCD spectroscopy allows resolve contributions of different elements into the total magnetic moment of a substance. In particular, the contribution of the Pr spins to the total magnetic moment of manganites was discussed earlier for the $Pr_{0.7}Ca_{0.3}MnO_3$ [20] and $Pr_{1-x}Pb_xMnO_3$ [21] compounds. XMCD spectra at the Mn K- and Pr L_2 - edges for the studied PSMO films are shown in Fig. 4. For the both compounds the obtained XMCD spectra at the Mn K- edge are in good agreement with the XMCD spectra for La-containing manganites, e.g., in [28]. We found no literature data on the XMCD spectrum at the Pr L_2 – edge for Pr-containing manganites. However, in our case, the observed spectra at the Pr L_2 – edge (Fig. 4) are similar to the L_2-edge spectrum of Eu in EuN [29].

The magnetic field dependences of the XMCD signal and the samples magnetization measured at T=90 K are shown in Fig. 5. The magnetic field dependences of the XMCD signal at the Mn K-edge (6553 eV) represent a symmetric hysteresis loops with the magnetic

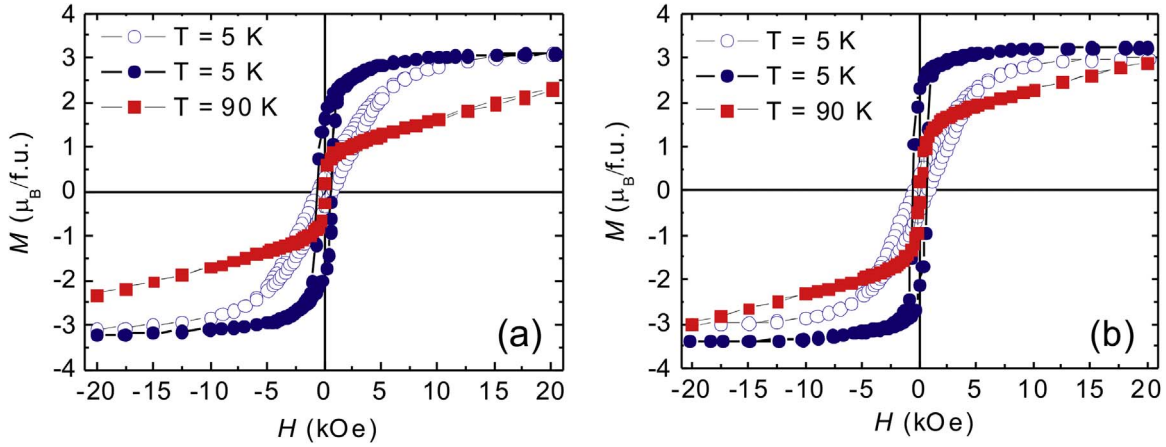

Fig. 2. Hysteresis loops for (a) $Pr_{0.8}Sr_{0.2}MnO_3$ and (b) $Pr_{0.6}Sr_{0.4}MnO_3$ films (150 and 130 nm in thickness, correspondingly) at T=5 K (circles) and 90 K (squares) in an external magnetic field parallel (closed symbols) and perpendicular (open symbols) to the film plane. The contribution of the substrate to the magnetization is subtracted.

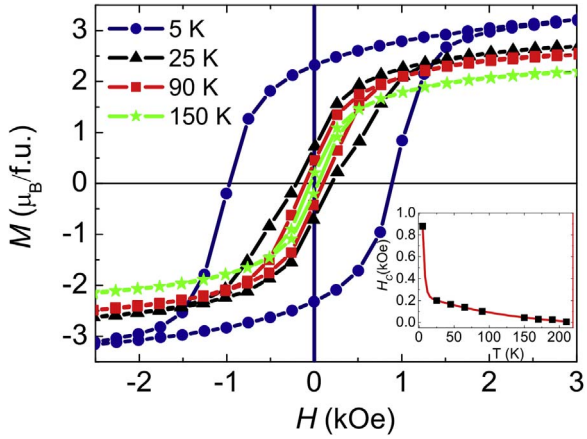

Fig. 3. Hysteresis loops for $Pr_{0.6}Sr_{0.4}MnO_3$ film (50 nm in thickness) in an external magnetic field parallel to the film plane at different temperatures. Inset: temperature dependence of H_C for the same sample.

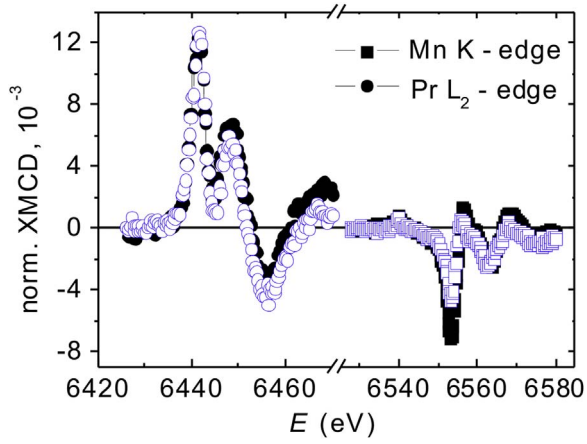

Fig. 4. XMCD spectra at the Pr L_2- and Mn K- edges for the $Pr_{0.8}Sr_{0.2}MnO_3$ (open symbols) and $Pr_{0.6}Sr_{0.4}MnO_3$ (closed symbols) films. T=90 K, magnetic field H =10 kOe.

saturation field, H_s, ~2 kOe and H_C~400 Oe for the $Pr_{0.8}Sr_{0.2}MnO_3$ film (Fig. 5a) and H_s~2 kOe and H_C~300 Oe for the $Pr_{0.6}Sr_{0.4}MnO_3$ film (Fig. 5b). The magnetic field dependences of the XMCD signal at the Pr L_2-edge (6441 eV) obtained for both PSMO compounds represent the symmetric curves passing through zero (inserts in Fig. 5), which involves the linear portion where the signal sharply increases in relatively low fields and the portion resembling the approach to saturation. The second portion can be associated with the Van Vleck paramagnetism of Pr^{3+} ions, which could explain the shape of the magnetization curve of the samples at temperatures above 25 K. Returning to Fig. 5., one can see that the magnetization curves at T=90 K do not saturate in the applied field up to 20 kOe and the shape of whole magnetization curves looks like a sum of the XMCD curves for Mn and Pr edges. The difference between H_C values obtained from the magnetization and XMCD can be due to the measurement conditions.

4. Discussion

To begin the analysis of the obtained experimental results, we would like to emphasize some features, specifically, the lower temperature of the magnetic phase transition, T_C, comparing to the results for the bulk stoichiometric single crystalline $Pr_{0.8}Sr_{0.2}MnO_3$ and $Pr_{0.6}Sr_{0.4}MnO_3$ samples, the difference between the FC and ZFC magnetization temperature dependences, hysteresis observed in the magnetization curves measured in the perpendicular geometry, the change of shape of the magnetization curves and the sharp H_C increase with the temperature decrease, and the XMCD signal dependence at the Mn K- and Pr L_2-edges on magnetic field.

The difference between the FC and ZFC temperature dependences of magnetization is typical of magnetically inhomogeneous systems, such as ensembles of superparamagnetic particles [30], nanocrystalline samples [31], spin glasses [32] and so on. For example, in nanocrystalline films, this difference can be related to the random distribution of the easy magnetization axes of crystallites. As was mentioned above, the investigated films consist of randomly oriented nanocrystals [23]. Upon cooling the films in a magnetic field, the magnetization direction in each crystallite is determined by the competition between the magnetic crystallographic anisotropy energy and Zeeman energy. In sufficiently strong magnetic fields, the magnetic moments of crystallites arrange along the field and the FC curve follows the spontaneous magnetization of a material. Upon cooling in zero fields, the magnetic moments align along the easy axis of each crystallite and a sample has no total magnetic moment, or this moment is smaller than that in the case of the FC mode. When the field is applied during heating, the magnetic moments of crystallites start adapting to the field direction, what leads to an increase in the total magnetization of the film. However, the spontaneous magnetization of the material decreases with increasing temperature. Thus, the competition between these processes results in the maximum appearance in the ZFC curve at temperature T_m. Generally, T_m can either coincide with T_{irr} or be lower than T_{irr}. Although this picture explains qualitatively the FC and ZFC temperature behavior of the investigated films magnetization, one can consider other mechanisms proposed in the current literature.

The similar difference was observed between the FC and ZFC curves for the $La_{0.7}Sr_{0.3}MnO_3$ [10,11] and $Pr_{0.7}Ca_{0.3}MnO_3$ [20] epitaxial films and was attributed by the authors to the spin-glass behavior of the samples. According to the spin glass theory, the temperature T_f at

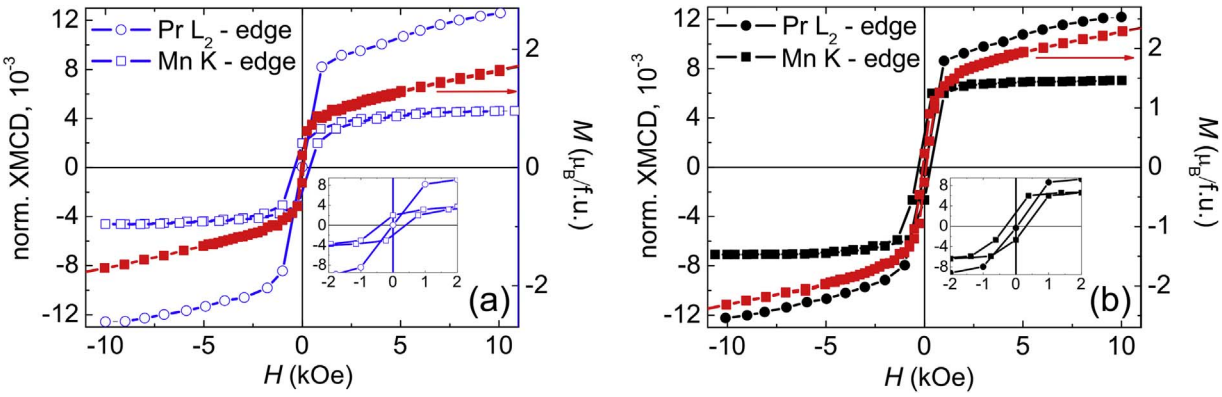

Fig. 5. Field dependences of the XMCD signal at the Pr L_2- edge (6441 eV) and Mn K- edge (6553 eV) for the $Pr_{0.8}Sr_{0.2}MnO_3$ (open symbols) and $Pr_{0.6}Sr_{0.4}MnO_3$ (closed symbols) films. T=90 K, magnetic field H= ± 10 kOe. Inserts: the same dependences on the scale. Magnetization curves at T=90 K are presented for comparison.

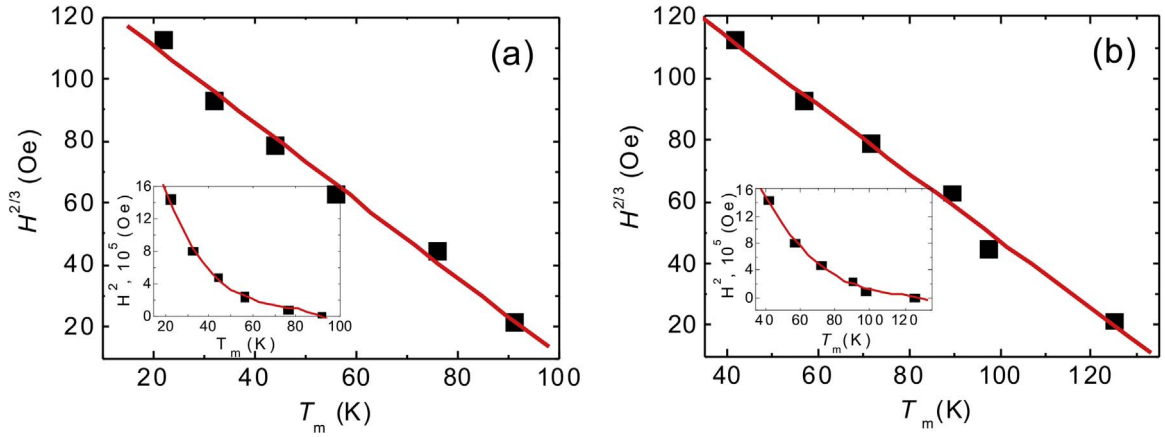

Fig. 6. T_m vs $H^{2/3}$and H^2 (insets) for (a) $Pr_{0.8}Sr_{0.2}MnO_3$ and (b) $Pr_{0.6}Sr_{0.4}MnO_3$ films (150 and 130 nm in thickness, correspondingly). The magnetic field is parallel to the film plane.

which all frustrated magnetic moments of a system become frozen depends on magnetic field H according to the power law $T_f = a + bH^n$. For the Ising spin system, n=2/3 and the T_f should be linear function of $H^{2/3}$ (so called the Almeida-Thouless line [33]). Namely this ratio between H and T_f was obtained in Ref. [34] for the $La_{0.7}Sr_{0.3}MnO_3$ film. For the Heisenberg spin system, n=2 and the linear dependence of T_f on H^2 should be observed. Fig. 6 shows the linear T_m dependence on $H^{2/3}$ for the PSMO films of both compositions. At the same time, T_m dependence on H^2 is clearly of the nonlinear character (insets in Fig. 6). Thus, one can identify the temperature T_m as the freezing temperature T_f of the Ising spin glass which realizes in PSMO films when cooling them in zero fields from the temperatures exciding T_C. Note, that A. Oleaga with co-authors investigating critical behavior of $Pr_{0.6}Sr_{0.4}MnO_3$ single crystals [35], have obtained the critical exponents corresponding to the 3D-Ising universality class and underlined the necessity of introducing magneto-crystalline anisotropy in the system to describe adequately its magnetic properties. They stated also that further studies concerning the magnetism of these systems should be undertaken in order to find a theoretical explanation for this anisotropy. Thus, to make unambiguous choice between mechanisms responsible for the different FC and ZFC thermomagnetic curves, the additional experiments are necessary which are in progress now.

Now turn to the hysteresis in the perpendicular magnetization curves and to strong increase of coercivity at low temperatures as both phenomena seem to be of the same origin. In the case of thin films, the difference in the magnetization behaviors at two mutually perpendicular external magnetic field orientations is due to the so called shape anisotropy that makes preferable the parallel films magnetic moment direction to the film surface. The demagnetizing magnetic field, H_d, prevents the magnetic moment to turn perpendicularly to the film plane (the values of the demagnetizing fields are given in Tables 2 and 3). For thin films $H_d = 4\pi M$. Thus, the magnetization curves with hysteresis and magnetic saturation at relatively low magnetic fields should be observed in the parallel magnetization geometry while without hysteresis curves with saturation at $H = H_d$ will take place in the case of magnetic film having the shape anisotropy only. Deviations from such behavior are associated with other types of magnetic anisotropy in a film. Nanocrystalline ferromagnets were investigated by many authors beginning with the best known work of E.C. Stoner and E.P. Wohlfarth [36] who showed that the hysteresis loop characteristics, coercivity and remnant magnetization, of heterogeneous magnetic materials including those consisting of small grains of different orientations were determined by the grains crystallographic and shape anisotropy, and stresses. The random orientation of the anisotropy easy axes of grains (nanocrystals) were the main condition of the model and the magnetic state of the whole system depended strongly on the competition between the local magnetic anisotropy and exchange energy [37]. For large grains, the magnetization can follow the easy axes direction in each nanocrystal, and the magnetization process is determined by the magneto crystalline anisotropy K_1 of the crystallites. For very small nanocrystals exchange interaction is dominated making all magnetic moments to be aligned parallel independently of the direction of the crystallites easy-axis. Evidently, the higher is the K_1 value the larger will be the role of the local anisotropy. In the case of very large grains or very high K_1 value, magnetization in each grain lies along the easy directions closest to the direction of the applied field and uniformly distributed within a cone with the spatial semi-vertex angle. After turning off the external field, the magnetic moments are oriented within this cone providing remnant magnetization, i.e., hysteresis. The angle decreases with the grain size or/and K_1 decrease. The K_1 temperature changes can cause different magnetization behavior in different temperature intervals.

Basing on the model described, one can associate the low temperature hysteresis loops observed both in parallel and perpendicular orientations of an external magnetic field and the sharp temperature of H_C with the local crystallographic anisotropy of a substance. K. Steenbeck with co-authors have studied temperature dependence of the magnetic anisotropy of the $La_{0.7}(Sr, Ca)_{0.3}MnO_3$ epitaxial films deposited to different substrates [38,39]. They have shown two types of anisotropies coexisting in films. (1) Biaxial anisotropy with easy axis ⟨110⟩ which can be described as a cubic crystal anisotropy of high enough value up to -10^{-4} J/m^3 at low temperatures; this anisotropy was nearly independent of the film thickness and the substrate nature, but depended extremely on the measurement temperature: it increases more than one order of value when temperature decreases from ~250–5 K. At that, the rate of the anisotropy increase upon temperature changed strongly when Sr was changed for Ca. (2) The uniaxial magnetic anisotropy which, practically, did not depend on temperature, but depended strongly on the substrate material and was ascribed to stresses at the boundary film-substrate because of mismatch between film and substrate crystal parameters. As far as the investigated films were nanocrystalline without any texture, we should take into account the shape anisotropy rather than the anisotropy associated with stresses. Thus, the shape anisotropy is responsible for the difference in the saturation field for the parallel and perpendicular magnetization (see Fig. 2), and the local crystallographic anisotropy is responsible for the hysteresis at the perpendicular magnetization and the low-temperature coercivity increase. If it is true, the H_C temperature dependence should reflect the temperature dependence of the crystallography anisotropy.

The low-temperature saturation of the magnetization curves of the PSMO films and the absence of the magnetic saturation at temperature above ~25 K are more difficult for the explanation. Effect of Pr ions on the magnetic properties of manganite can be considered as one of the

reasons of such changes. Since XMCD study of the PSMO samples reveals Van Vleck susceptibility of Pr^{3+} ions, the absence of the magnetic saturation in high magnetic fields we interpret as a consequence of the paramagnetic contribution of Pr ions. At that, the low-temperature saturation of the magnetization curves indicates on the ordering of Pr spins and their contribution to the total magnetization of the films.

To estimate the correspondence of the films magnetization value to that available in literature, comparing of our results seems to be reasonable with the results obtained by the other authors realizing magnetization measurements at the close conditions. Temperature magnetization dependence of the bulk polycrystalline $Pr_{0.6}Sr_{0.4}MnO_3$ samples synthesized by the conventional solid-state reaction method was obtained in the external magnetic field of 500 Oe (Fig. 1 in Refs. [40,41]. Magnetic moment at 4.2 K was shown to be equal to approximately 1.0 μ_B/f.u. (or 28 emu/g) and to 30 emu/g at 100 K. Analogous measurements were made for the polycrystalline bulk $Pr_{0.6}Sr_{0.4}MnO_3$ samples prepared with the same method in Ref. [42]. Magnetization value at 100 K was obtained to be equal to 0.75 μ_B/f.u. (or 21 emu/g). For the ceramic samples of $Pr_{0.8}Sr_{0.2}MnO_3$ prepared also using the standard solid state reaction method, magnetic moment in the interval of 4.2–100 K was about 0.65 μ_B/f.u. (or 18 emu/g) in magnetic field 500 Oe [43]. At the same time, for the nanometric granular polycrystalline $Pr_{0.8}Sr_{0.2}MnO_3$ samples synthesized by chemical pyrophoric reaction process, magnetic moment was about 1.4 μ_B/f.u. (or 40 emu/g) in magnetic field 100 Oe [44]. This overview demonstrates significant differences between the results of different authors on the samples of the same nominal composition. Thus, our estimations of the studied films magnetic moment do not contradict the data available in the current literature. Note that the data of the magnetic measurements do not allow judging about the role of Pr ions in the formation of the compound magnetic moment. According to the neutron diffraction data, the Pr spins in $Pr_{1-x}Ca_xMnO_3$ ($0.2 \leq x \leq 0.3$) have a net moment of 0.6 μ_B below 60 K [45]. If Pr ions ordering occur indeed in $Pr_{1-x}Sr_xMnO_3$, this phenomenon should take place also for all PSMO samples.

The induced magnetic moment in the Pr below 25 K requires a separate discussion which is beyond the scope of the presented work and will be published later. Note that the magnetic properties of compounds containing *3d* transition metals and *4f* rare-earth metals have been investigated for a long time [46–49]. Most of the studies in this field were aimed at clarifying the role of the rare-earth *5d* states in the *3d-4f* interaction. It was found that the magnetic ordering in these compounds is related to the indirect exchange between the spin polarized *4f* orbitals and *5d* orbitals, which, in turn, are coupled by the direct exchange with the spin polarized *3d* orbitals of a transition metal. Some authors mentioned possible coupling between Pr *4f* and Mn *3d* spins in studying the magnetic and transport properties of praseodymium manganites [20,21].

The reasons of the low T_C values of the samples are currently not clear. According to the literature, strong enough T_C changes were observed for the non-stoichiometric manganites both bulk and thin films [31,43,50–52]. However, in our case, preliminary analysis of the studied samples showed that their chemical composition corresponded to the claimed stoichiometry. It is worth noting that in these samples the MCD signal was observed at temperatures up to 300 K for $Pr_{0.6}Sr_{0.4}MnO_3$ and 170 K for $Pr_{0.8}Sr_{0.2}MnO_3$. This issue requires further studies, using more sensitive methods, for example, the magnetic resonance.

5. Conclusions

The PSMO films magnetic properties were studied based on the static magnetic and X-ray MCD measurements. Comparison of ZFC and FC magnetization dependences on temperature for the both film compositions showed a behavior typical of magnetically inhomogeneous media with maximum in the ZFC curve at certain temperature T_m. The temperature T_m depended on the value of the external magnetic field applied in the measurement process. The $T_m(H)$ dependence followed to the Almeida-Thouless low what allowed considering the possibility of the spin glass behavior of the samples subjected to ZFC. Other mechanism associated with the crystallographic anisotropy was considered too.

The character of the magnetization field dependences changed drastically with the temperature increase. The hysteresis loops at T=5 K were observed at two mutually perpendicular orientations of the external magnetic field relative to the film plane with the saturation magnetization of 2.46–3.24 μ_B/f.u. and the coercivity of 424–886 Oe in dependence on the film thickness. This shape of the low-temperature loops and a sharp coercivity decrease with increasing temperature are associated with the high local crystallographic anisotropy in the low temperature interval and its decrease with the temperature increase. The change of the shape of the magnetization curves at temperature above ~25 K was attributed to Van Vleck contribution from Pr^{3+} ions.

The whole set of the results obtained induces one to come to the conclusion that, contrary to the sufficient difference between magneto-optic properties of PSMO films with x=0.2 and 0.4 [23], the magnetization dependences on temperature and magnetic field of the same films have more similarities than differences, excluding the difference in the magnetic transition temperature corresponding to that in the bulk samples.

Acknowledgments

The work was supported by the Russian Foundation for Basic Research, Project no's. 14-02-01211, 16-32-00209 mol_a, and also the Grant of the President of the Russian Federation no. NSh-7559.2016.2, and the Ministry of Education and Science of the Russian Federation, Project no. 1362.

References

[1] A.P. Ramirez, Colossal magnetoresistance, J. Phys.: Condens. Matter. 9 (1997) 8171–8199.
[2] A.-M. Haghiri-Gosnet, J.-P. Renard, CMR manganites: physics, thin films and devices, J. Phys. D: Appl. Phys. 36 (2003) R127–R150.
[3] J.M.D. Coey, M. Viret, S. von Molnar, Mixed-valence manganites, Adv. Phys. 48 (1999) 167–293.
[4] O. Chmaissem, B. Dabrowski, S. Kolesnik, J. Mais, J.D. Jorgensen, S. Short, Structural and magnetic phase diagrams of $La_{1-x}Sr_xMnO_3$ and $Pr_{1-y}Sr_yMnO_3$, Phys. Rev. B 67 (2003) 094431.
[5] N.V. Volkov, Spintronics: manganite-based magnetic tunnel structures, Phys.-Uspekhi 55 (2012) 250–269.
[6] Liu Yu-Kuai, Yin Yue-Wei, Li Xiao-Guang, Colossal magnetoresistance in manganites and related prototype devices, Chin. Phys. B. 22 (2013) 087502.
[7] H.A. Kramers, L'interaction entre les atomes magnétogènes dans un cristal paramagnétique, Physica 1 (1934) 182–192.
[8] C. Zener, Phys. Rev. 81 (1951) 440.
[9] C. Zener, Phys. Rev. 82 (1951) 403.
[10] S.V. Trukhanov, A.V. Trukhanov, H. Szymczak, Effect of magnetic fields on magnetic phase separation in anion-deficient manganite $La_{0.70}Sr_{0.30}MnO_{2.85}$, Low. Temp. Phys. 37 (2011) 465–469.
[11] V.A. Sirenko, V.V. Eremenko, Irreversibility and anisotropy of the low-temperature magnetization in manganites. Spin-glass polyamorphism, Low Temp. Phys. 40 (2014) 179–184.
[12] W. Boujelben, A. Cheikh-rouhou, M. Eellouze, J.C. Joubert, Synthesis, x-ray, magnetic and electrical studies of substituted (Pr, Sr)MnO_3 perovskites, J. Phase Transit. 71 (2000) 127–141.
[13] N. Rama, V. Sankaranarayanan, M.S. Ramachandra Rao, Role of double exchange interaction on the magnetic and electrical properties of $Pr_{0.8}Sr_{0.2}MnO_3$ ferromagnetic insulating manganite, J. Appl. Phys. 99 (2006) 08Q315.
[14] S. Rößler, S. Harikrishnan, U.K. Rößler, C.M.N. Kumar, S. Elizabeth, S. Wirth, Ferromagnetic transition and specific heat of $Pr_{0.6}Sr_{0.4}MnO_3$, Phys. Rev. B 84 (2011) 184422.
[15] D.V. Maheswar Repaka, T.S. Tripathi, M. Aparnadevi, R. Mahendiran, Magnetocaloric effect and magneto thermo power in the room temperature ferromagnet $Pr_{0.6}Sr_{0.4}MnO_3$, J. Appl. Phys. 112 (2012) 123915.
[16] R. Thaljaoui, K. Pekala, M. Pekala, W. Boujelben, J. Szydlowska, J.-F. Fagnard, P. Vanderbemden, A. Cheikhrouhou, Magnetic susceptibility and electron magnetic resonance study of monovalent potassium doped manganites $Pr_{0.6}Sr_{0.4-x}K_xMnO_3$, J. Alloy. Compd. 580 (2013) 137–142.

[17] R. Thaljaoui, W. Boujelben, M. Pekala, K. Pekala, J. Antonowicz, J.-F. Fagnard, Ph Vanderbemden, S. Dabrowska, J. Mucha, Structural, magnetic and magneto-transport properties of monovalent doped manganite Pr0.55K0.05Sr0.4MnO3, J. Alloy. Compd. 611 (2014) 427–432.
[18] F. Elleuch, M. Triki, M. Bekri, E. Dhahri, E.K. Hlil, A-site-deficiency-dependent structural, magnetic and magnetoresistance properties in the $Pr_{0.6}Sr_{0.4}MnO_3$ manganites, J. Alloy. Comp. 620 (2015) 249–255.
[19] T. Kimura, S. Ishihara, H. Shintani, T. Arima, K.T. Takahashi, K. Ishizaka, Y. Tokura, Distorted perovskite with e_g^1 configuration as a frustrated spin system, Phys. Rev. B 68 (2003) 060403(R).
[20] Joonghoe Dho, W.S. Kim, E.O. Chi, N.H. Hur, S.H. Park, H.-C. Ri, Colossal magnetoresistance in perovskite manganite induced by localized moment of rare earth ion, Solid State Commun. 125 (2003) 143–147.
[21] B. Padmanabhan, Suja Elizabeth, H.L. Bhat, S. Rößler, K. Dörr, K.H. Müller, Crystal growth, transport and magnetic properties of rare-earth manganite $Pr_{1-x}Pb_xMnO_3$, J. Magn. Magn. Mater. 307 (2006) 288–294.
[22] S. Rößler, S. Harikrishnan, U.K. Rößler, Suja Elizabeth, H.L. Bhat, F. Steglich, S. Wirth, Interacting magnetic sublattices and ferrimagnetism in Sr-doped $DyMnO_3$, J. Phys.: Conf. Ser. 200 (2010) 012168.
[23] I. Edelman, Yu Greben'kova, A. Sokolov, M. Molokeev, A. Aleksandrovskiy, V. Chichkov, N. Andreev, Y. Mukovskii, Visible magnetic circular dichroism spectroscopy of the $Pr_{0.8}Sr_{0.2}MnO_3$ and $Pr_{0.6}Sr_{0.4}MnO_3$ thin films, AIP Adv. 4 (2014) 057125.
[24] W. Kuch, X-ray magnetic circular dichroism for quantitative element-resolved magnetic microscopy, Physica Scr. 109 (2004) 89–95.
[25] Y. Hoshi, M. Kojima, M. Naoe, S.-I. Yamanaka, Preparation of permalloy films using facing-type targets and a high-rate and low-temperature sputtering method, Electron. Commun. Jpn. Part. I.V. 65 (1982) 91–98.
[26] E.A. Antonova, V.L. Ruzinov, S.Yu Stark, V.I. Tchitchkov, Superconducting YBCO films by facing targets, Supercond. Phys. Chem. Technol. 4 (1991) 1624–1629.
[27] Y.E. Greben'kova, A.E. Sokolov, E.V. Eremin, I.S. Edel'man, D.A. Marushchenko, V.I. Zaikovskii, V.I. Chichkov, N.V. Andreev, Y.M. Mukovskii, Magnetization and magnetic circular dichroism of $La_{0.7}Sr_{0.3}MnO_3$/YSZ polycrystalline films, Phys. Sol. State 55 (2013) 842–849.
[28] G. Subias, J. Garcia, M.C. Sanchez, Mn K-edge XMCD study of the mixed-valence state of Mn-based molecular nanomagnets, AIP Conf. Proc. 882 (2007) 783–785.
[29] B.J. Ruck, H.J. Trodahl, J.H. Richter, J.C. Cezar, F. Wilhelm, A. Rogalev, V.N. Antonov, Binh Do Le, C. Meyer, Magnetic state of EuN: X-ray magnetic circular dichroism at the EuM_4,5 and L_2,3 absorption edges, Phys. Rev. B 83 (2011) 174404.
[30] R.W. Chantrell, N.S. Walmsley, J. Gore, M. Maylin, Theoretical studies of the field-cooled and zero-field cooled magnetization of interacting fine particles, J. Appl. Phys. 85 (1999) 4340.
[31] W. Boujelben, A. Cheikh-Rouhou, J. Pierre, J.C. Joubert, Ferromagnetism in the lacunar (Pr, Sr)MnO3 perovskite manganites, Physica B 321 (2002) 37–44.
[32] K. Binder, A.P. Young, Spin-glasses – experimental facts, theoretical concepts, and open questions, Rev. Mod. Phys. 58 (1986) 801–976.
[33] J.R.L. De Almeida, D.J. Thouless, Stability of the Sherrington-Kirkpatrick solution of a spin glass model, J. Phys. A: Math. Gen. 11 (1978) 983–990.
[34] A.G. Lehmann, C. Sanna, F. Congiu, G. Concas, L. Maritato, Pure ferromagnetism vs. re-entrant spin glass behavior in epitaxial $La_{0.7}Sr_{0.3}MnO_3$ on $SrTiO_3$(001) and $LaAlO_3$(001): the role of the substrate structural transition, Phys. Stat. Sol. B 246 (2009) 1948–1955.
[35] A. Oleaga, A. Salazar, M. Ciomaga Hantean, G. Balakrishnan, Three-dimensional Ising critical behavior in $R_0.6Sr_{0.}4MnO_3$ (R=Pr, Nd) manganites, Phys. Rev. B 92 (2015) 024409.
[36] E.C. Stoner, E.P. Wohlfarth, A mechanism of magnetic hysteresis in heterogeneous alloys, Philos. Trans. Roy. Soc. A 240 (1948) 599.
[37] G. Herzer, Grain size dependence of coercivity and permeability in nanocrystalline ferromagnets, IEEE Trans. Magn. 26 (1990) 1397–1402.
[38] K. Steenbeck, R. Hiergeist, Magnetic anisotropy of ferromagnetic $La_{0.}7(Sr,Ca)_0.3MnO_3$ epitaxial films, Appl. Phys. Lett. 75 (1999) 1778.
[39] K. Steenbeck, T. Habisreuther, C. Dubourdieu, J.P. Sénateur, Magnetic anisotropy of ferromagnetic $La_0.7Sr_{0.}3MnO_3$ epitaxial thin films: dependence on temperature and film thickness, Appl. Phys. Lett. 80 (2002) 3361.
[40] S. Zemni, M. Baazaoui, J. Dhahri, H. Vincent, M. Oumezzine, Above room temperature magnetocaloric effect in perovskite $Pr_0.6Sr_0.4MnO_3$, Mater. Lett. 63 (2009) 489–491.
[41] S. Hcini, S. Zemni, M. Baazaoui, J. Dhahri, H. Vincentb, M. Oumezzine, Critical phenomena in $Pr_0.6Sr_0.4MnO_3$ perovskite manganese oxide, Solid State Sci. 14 (2012) 644–649.
[42] M.D. Daivajna, N. Kumar, V.P.S. Awana, B. Gahtori, J.B. Christopher, S.O. Manjunath, K.Z. Syu, Y.K. Kuod, A. Rao, Electrical, magnetic and thermal properties of $Pr_0.6$-$xBi_{x}Sr_0.4MnO_3$ manganites, J. Alloy. Compd. 588 (2014) 406–412.
[43] W. Cheikh-Rouhou Koubaa, M. Koubaa, W. Boujelben, A. Cheikhrouhou, A.-M. Haghiri-Gosnet, J.-P. Renard, Deficiency effects upon the physical properties of $Pr_0.8Sr_0.2MnO_3$ manganite oxide, Phys. Stat. Sol. C 3 (2006) 3206–3210.
[44] P.T. Das, A. Taraphder, T.K. Nath, Magnetic, electronic and magneto-transport studies of ferromagnetic insulating under doped $Pr_0.8Sr_0.2MnO_3$ manganite on nanometric grain size modulation, AIP Conf. Proc. 1349 (2011) 383.
[45] Z. Jirak, S. Krupicka, Z. Simsa, M. Dlouha, S. Vratislav, Neutron diffraction study of $Pr_{1-x}CaxMnO_3$ perovskites, JMMM 53 (1985) 153–166.
[46] B.N. Harmon, A.J. Freeman, Spin-polarized energy-band structure, conduction electron polarization, spin densities, and the neutron magnetic form factor of ferromagnetic gadolinium, Phys. Rev. B 10 (1974) 1979–1993.
[47] G. Schutz, M. Knulle, R. Wienke, W. Wilhelm, W. Wagner, P. Kienle, R. Frahm, Spin-dependent photo absorption at the L-edges of ferromagnetic Gd and Tb metal, Z. Phys, B: Condens. Matter 73 (1988) 67–75.
[48] L.T. Baczewski, D. Givord, J.M. Alameda, B. Dieny, J.P. Nozieres, J.P. Rebouillat, J.J. Prejean, Magnetism in rare-earth-transition metal systems. Magnetization reversal and ultra-high susceptibility in sandwiched thin films based on rare-earth and cobalt alloys, Acta Phys. Polonica A 83 (1993) 629–641.
[49] M.A. Laguna-Marco, J. Chaboy, C. Piquer, Experimental determination of the R(5d)-T(3d) hybridization in rare-earth intermetallics, Phys. Rev. B 77 (2008) 125132.
[50] M. Koubaa, W. Prellier, R. Soulimane, W. Boujelben, A. Cheikh-Rouhou, Ph Lecoeur, A.-M. Haghiri-Gosnet, Role of A-site deficiency in the magneto-transport properties of $Pr_{0.7}Sr_{0.3}MnO_3$ relaxed films, Eur. Phys. J. 47 (2005) 29–35.
[51] H.L. Ju, J. Gopalakrishnan, J.L. Peng, Q. Li, G.C. Xiong, T. Venkatesan, R.L. Greene, Dependence of giant magnetoresistance on oxygen stoichiometry and magnetization in polycrystalline $La_{0.67}Ba_{0.33}MnO_3$, Phys. Rev. B 51 (1995) 6143–6146.
[52] G.F. Wang, Z.R. Zhao, L.R. Li, X.F. Zhang, Effect of non-stoichiometry on the structural, magnetic and magnetocaloric properties of $La_{0.67}Ca_{0.33}Mn_{1-\delta}O_3$ manganites, J. Magn. Magn. Mater. 397 (2016) 198–204.